Investigation of UWB-IMU Sensor Fusion for Indoor Navigation with DoE

1st Şehrinaz DURMUŞ
Mechatronics Engineering Department
Marmara University
Istanbul,Turkey
sehrinazdurmus@marun.edu.tr

2nd Uğur DEMİR
Mechatronics Engineering Department
Marmara University
Istanbul,Turkey
udemir@marmara.edu.tr

3rd Gazi AKGÜN
Mechatronics Engineering Department
Marmara University
Istanbul,Turkey
gazi.akgun@marmara.edu.tr

4th Alper YILDIRIM
Mechatronics Engineering Department
Marmara University
Istanbul,Turkey
yildirim.alper@marmara.edu.tr

2023 Innovations in Intelligent Systems and Applications Conference (ASYU) | 979-8-3503-0659-0/23/$31.00 ©2023 IEEE | DOI: 10.1109/ASYU58738.2023.10296828

***Abstract*—This study presents an evaluation of the optimal parameter configuration for Ultra-Wide Band (UWB) - Inertial Measurement Units – (IMU) based sensor fusion for indoor localization in Non-Line-of-Sight (NLOS) environments. The study employs the least squares method to predict position using UWB technology. Subsequently, sensor fusion techniques combining UWB and IMU are employed, utilizing the Extended Kalman Filter (EKF) and Unscented Kalman Filter (UKF) algorithms to enhance position estimation. To mitigate the effects of noise in IMU data, a high-pass filter is applied before feeding the data into the EKF and UKF. The experimental findings are then evaluated using Design of Experiment (DoE) techniques, and the optimal parameter configurations are analysed using linear regression. This study provides insight into the parameter settings that yield improved accuracy and robustness in UWB-IMU sensor fusion for indoor localization in NLOS scenarios.**

Keywords— Design of Experiment, Indoor Navigation, Sensor Fusion, UWB, IMU

I. INTRODUCTION

Nowadays, indoor positioning systems offer significant advantages in detecting the positions of individuals, equipment, and other objects [1]. Various methods for indoor positioning exist, [2] including Wi-Fi, 5G, UWB, and LTE [3] radio-based positioning techniques. Furthermore, advanced techniques such as image processing combined with camera and LIDAR fusion are utilized. However, these techniques and tools encounter limitations related to obstacles, geometrical features and hardware-based constraints, particularly in singular usage scenarios.

In this study, radio-based Ultra-Wide Band (UWB) technology is preferred for indoor positioning due to its superior advantages, including low energy consumption, cost-effectiveness, high accuracy, multipath data transmission, higher bandwidth data transmission, and low latency in the picosecond range [3-5]. UWB technology, employing the IEEE 802.15.4 protocol [6], utilizes radio frequency waves to deliver precise positioning with short pulses, minimizing error accumulation. It offers a bandwidth of 500 MHz [1,6,7]. and faster data speeds compared to technologies like Bluetooth. Despite the many advantages of UWB positioning, NLOS multipath effects caused by environmental conditions can result in inaccurate measurements[1,6].

Another commonly used technique for positioning is the Inertial Measurement Unit (IMU) [8]. Inertial navigation relies on Newton's laws of physics and is influenced by gravity. The IMU sensor integrates acceleration measurements to calculate changes in speed and position relative to initial conditions [9]. A typical IMU consists of three gyroscopes for angular positions and three accelerometers for accelerations. Position calculations are derived by double integrating the acceleration measurements. Consequently, linear, and angular values require calibration, and even after calibration, they are susceptible to noise, leading to cumulative errors over time.

The combined use of UWB and IMU sensors mitigates drawbacks such as multipath effects, noise, and calibration issues, enabling precise and reliable positioning. In this study, the fusion of UWB and IMU sensors is investigated using Extended Kalman Filter (EKF) and Unscented Kalman Filter (UKF) algorithms. A high-pass filter is employed to remove noise from the IMU data before feeding it into the EKF and UKF algorithms. To analyse and evaluate the configuration parameters of the sensor fusion setup, Design of Experiments (DoE) techniques such as Taguchi and Box-Behnken Design (BBD) are employed. Subsequently, the optimal parameter configuration is determined using linear regression based on the DoE results.

II. SENSOR FUSION AND OPTIMIZATION

A. Coordinate transformation with IMU

The IMU is capable of detecting centrifugal forces caused by gravity and the Earth's rotation. To determine the forces sensed by the IMU, it is essential to ascertain the tilt between the platform on which the sensor is mounted and the local coordinates. Thus, the angular position data provided by gyroscopes becomes crucial [9]. Consequently, it is necessary to transform the IMU values to the navigation coordinate system where the UWB anchors are positioned [5]. This coordinate transformation is accomplished using the ZYX Euler angle set, as described by equations (1) and (2), where 'c' denotes cosine and 's' denotes sine.

$$C_n^b=\begin{bmatrix} c\alpha c\beta & c\alpha s\beta s\gamma - s\alpha c\gamma & c\alpha s\beta c\gamma + s\alpha s\gamma \\ s\alpha c\beta & s\alpha s\beta s\gamma + c\alpha c\gamma & s\alpha s\beta c\gamma - c\alpha s\gamma \\ -s\beta & c\beta s\gamma & c\beta c\gamma \end{bmatrix} \quad (1)$$

$$R_n^b=[R_t]^T * R_a \quad (2)$$

R_t is the rotation matrix of tag. And R_a is the anchor rotation matrix.

$$a^n= R_n^b * a^b \quad (3)$$

In (3), a^b refers the acceleration values in body frame, a^n refers the acceleration values in navigation frame.

B. Distance Measurement and Positioning with UWB

In UWB-based positioning, the distance between the tag and anchor is determined using the time of flight (ToF) method, which relies on two-way communication. The communication process begins with the tag sending a poll message to the anchor devices. The anchors respond with a response message, and the communication is finalized with a tag-final message, completing the handshaking process. The round trip time (RTT) is calculated by taking the difference between the timestamps of the sent messages [1,3].

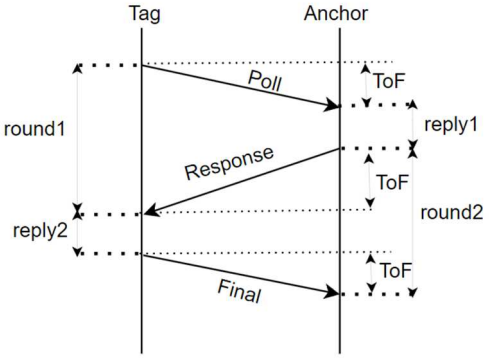

Fig. 1. TWR Communication

$$ToF=\frac{((round1-reply1)+(round2-reply2))}{4} \quad (4)$$

$$d = ToF*C \quad (5)$$

The distance between the tag and the anchor is calculated with (4). Where, C ≈ 299,792,458 m/s is the speed of light [5]. d is the distance between the tag and the anchor.

There are two methods available to estimate the position based on the distances obtained through the TWR communication between the tag and anchor devices. These methods include trilateration and the least squares method. In this study, the position estimation is performed using the least squares method, as described in equation (6). To calculate the position of a tag using the least squares method, it is essential to measure the distances from at least three anchors [1].

$$(x,y)=\text{argmin}(x,y)\ \sum_{i=1}^{k} (di-||(x,y)-Ai||)^2 \quad (6)$$

C. Extended Kalman Filter

For EKF, IMU data is used in prediction equations. UWB data is used in updating equations. The system model is given in (7).

$$x_k=[x_k\ y_k\ V_k^x\ V_k^y] \quad (7)$$

Where, x_k and y_k are the state positions on x-axis and y-axis, respectively. V_k^x and V_k^y are the state speeds on x-axis and y-axis, respectively. The next state is defined in (8), (9) and (10). Where, A is the state transition matrix. B is an input matrix. w_k is a process noise vector. u_k is a vector that represents the acceleration on the x and y axes expressed in the navigation frame. Q is the states covariance matrix, which refers to the process noise.

$$x_{k+1}=Ax_k+Bu_k+ w_k \quad (8)$$

$$A=\begin{bmatrix} 1 & 0 & \Delta t & 0 \\ 0 & 1 & 0 & \Delta t \\ 0 & 0 & 1 & 0 \\ 0 & 0 & 0 & 1 \end{bmatrix} \quad B=\begin{bmatrix} \frac{\Delta t^2}{2} & 0 \\ 0 & \frac{\Delta t^2}{2} \\ \Delta t & 0 \\ 0 & \Delta t \end{bmatrix} \quad (9)$$

$$u= a^n\ ,\ w_k \sim N(0,Q) \quad (10)$$

The obtained measurements from the UWB sensor generate the observation matrix. d_k^i is the measured distance from UWB. i and k are substituted as anchor and time, respectively. The observation matrix is given in (14),

$$z_k= \left[d_k^1 \ldots .. d_k^i\right]^T \quad (11)$$

$$z_k=H_k x_k+ v_k \quad (12)$$

$$v_k \sim N(0,R) \quad (13)$$

$$h_k=\begin{bmatrix} \sqrt{(x_k-A_{x,1})^2+(y_k-A_{y,1})^2} \\ \vdots \\ \sqrt{(x_k-A_{x,i})^2+(y_k-A_{y,i})^2} \end{bmatrix} \quad (14)$$

Where, z_k is the measurement vector. h_k refers to the observation matrix. R refers the measurement noise. $A_{x,i}$ and $A_{y,i}$ refer to the x and y points of the UWB anchor at the navigation frame. The H_k is Jacobian matrix which is obtained by taking partial derivatives of h_k matrix with respect to x and y.

$$H_k=\begin{bmatrix} \frac{(x_k-A_{x,1})}{\sqrt{(x_k-A_{x,1})^2+(y_k-A_{y,1})^2}} & \frac{(y_k-A_{y,1})}{\sqrt{(x_k-A_{x,1})^2+(y_k-A_{y,1})^2}} \\ \vdots \\ \frac{(x_k-A_{i,1})}{\sqrt{(x_k-A_{i,1})^2+(y_k-A_{i,1})^2}} & \frac{(y_k-A_{i,1})}{\sqrt{(x_k-A_{i,1})^2+(y_k-A_{i,1})^2}} \end{bmatrix} \quad (15)$$

D. Unscented Kalman Filter

UKF is based on unscented transformation (UT) which is an approach to predicting the statistics of random variable. For UKF, the points are used to capture the real covariance and mean of random variables, unlike from EKF. Calculating the

Jacobian matrix is not necessary for UKF. Instead of the Jacobian matrix, sigma points and weights are calculated [7]. The process equations of UKF are given in (16), (17), and (18). In this study, α=0.001, β=2, λ=0 was used.

System initialization:

$$\begin{cases} \hat{x}_0=E[x_0] \\ P_0=E\left[(x-\hat{x}_0)(x-x_0)^T\right] \end{cases} \quad (16)$$

State estimation:

$$\begin{cases} x_k^0=\hat{x}_k \\ x_k^i=\hat{x}_k+\left(\sqrt{(n+\lambda)P_k}\right)_i \text{ , } i=1,2,\ldots.n \\ x_k^{i+n}=\hat{x}_k-\left(\sqrt{(n+\lambda)P_k}\right)_i \text{ , } i=1,2,\ldots.2n \end{cases} \quad (17)$$

Weight:

$$\begin{cases} W_0^m=\frac{\lambda}{(n+\lambda)} \\ W_0^c=\frac{\lambda}{(n+\lambda)}+1-\alpha^2+\beta \\ W_i^m=W_i^c=\frac{\lambda}{2(n+\lambda)} \text{ , } i=1,\ldots.,2n \end{cases} \quad (18)$$

E. Design of Experiment

Taguchi's design of experiment method (DoE) provides a reduction of assessment duration of system parameters. Besides, the DoE approach allows to determine prioritization of the system parameters. Therefore, it enables to avoid long iterative analysis time and higher cost [10-14].

III. MATERIALS METHODS

A. Application of Experimental Design

In this section, DoE is dealt with three parameters which are UWB anchor number, UWB sample time, and IMU sample time. For these parameters, three levels are determined. The determined parameters levels are given in Table I.

TABLE I. LEVELS OF SYSTEM PARAMETERS

Parameters	Level 1	Level 2	Level 3
Number of UWB Anchor	4	5	6
UWB Period (Hz)	2	5	10
IMU Period (Hz)	25	50	100

Table II shows the orthogonal array selection matrix for DoE. Here, the L9 experiment array is appropriate for three parameters and three levels.

TABLE II. ORTHOGONAL EXPERIMENTS MATRIX

		Number of Parameters		
		2	3	4
Number of Parameter Level	2	L4	L4	L8
	3	L9	L9	L9

DoE are given in Table III, which is arranged according to the L9 experiment array.

TABLE III. DESIGN OF EXPERIMENTS (L9)

Experiment	Number of UWB Anchor	UWB Period (Hz)	IMU Period (Hz)
1	4	2	25
2	4	5	50
3	4	10	100
4	5	2	50
5	5	5	100
6	5	10	25
7	6	2	100
8	6	5	25
9	6	10	50

B. Hardware and Test Environment

In this study, DWM1001 transceiver, DWM1001 development board of Qorvo, which includes NRF52832 Arm Cortex M4F MCU are used for the distance measurement of the anchor-tag. As shown in Fig. 2, USFSMAX AHRS module is connected to the DWM1001 development board to obtain real-time orientation. USFSMAX module is a motion co-processor that is connected to a three axis gyroscope, three axis accelerometer, and three axis magnetometer outputs to obtain the direction of the device. This module is working via I^2C dependent and provides Euler angles.

As shown in Fig. 3, UWB anchors are positioned at the corners of the test zone, which features a column barrier causing a non-line-of-sight(NLOS) scerario. The configuration of UWB 4,5 and 6, as specified in Table III, is utilized. The dimension of the test zone is 5m x 16m.

As shown in Fig. 4, the UWB tag is positioned on the table. The distance measurement obtained from UWB are logged in the read-only memories (ROMs) of each anchor device. IMU measurements are logged from the tag, and transferred to the computer through a serial connection. One of the anchors is selected as the base of the coordinate system while the positions of the remaining anchors are calculated using Powell's minimization algorithm.

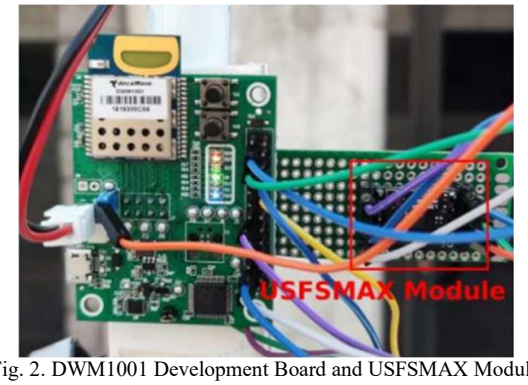

Fig. 2. DWM1001 Development Board and USFSMAX Module

Fig. 3. Position of UWB Anchors

Fig. 4. Placement of UWB Tag

C. *Processing of Data*

Firstly, the estimation of the position with UWB is realized by using the least squares method. Subsequently, coordinate transformation of the IMU data is conducted to estimate the position through sensor fusion of UWB and IMU. The u (control matrix) values obtained as a result of the coordinate transformation are processed and filtered with a high-pass filter. In the final step for the estimation of the position, EKF and UKF are used.

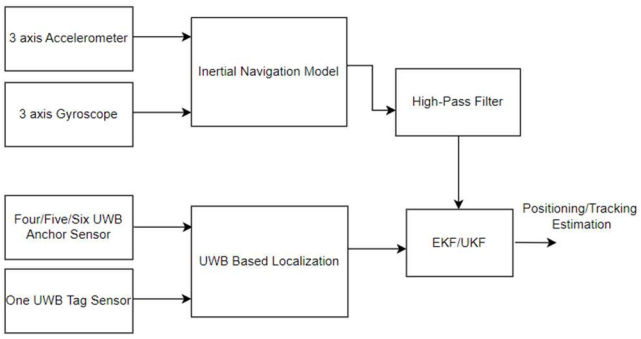

Fig. 5. Data Flow for Sensor Fusion

IV. RESULT

In NLOS conditions, the obtained data from DoE is fed to EKF and UKF. Considering the sensor fusion algorithm, the obtained data of the instant position and reference position are compared in terms of the MAPE (Mean Absolute Percentage Error) results which are given in Table IV.

TABLE IV. MAPE RESULTS

Experiment	EKF		UKF	
	MAPEX%	MAPEY%	MAPEX%	MAPEY%
1	23,0797	5,7058	21,7199	3,5488
2	24,0823	4,6873	23,4181	3,4743
3	16,0828	4,6573	15,9104	3,9217
4	19,0585	7,2480	17,2864	3,9950
5	12,9946	6,4179	11,8463	4,7551
6	10,6293	4,9280	10,5755	4,9437
7	27,5114	11,6782	25,6806	7,1005
8	31,0688	6,1595	29,1874	5,9583
9	28,8524	7,0631	27,3297	17,0983

The Box-Behnken design (BBD) method is used to calculate the optimal configuration for the parameters. It is observed that the configuration with the number of anchors '5', UWB period '10Hz' and the IMU period '100Hz' gives the optimal results. For the linear regression, the fitted equations for the x and y axes are given in (19) and (20).

$$FEKFX = \beta_{0k} + ANC * \beta_{1k} + UWB * \beta_{2k} + IMU * \beta_{3k} + ANC * UWB * \beta_{4k} + ANC * IMU * \beta_{5k} + ANC^2 * \beta_{6k} + UWB^2 * \beta_{7k} + IMU^2 * \beta_{8k} + \varepsilon_{0k} \quad (19)$$

$$FEKFY = \beta_{0k} + ANC * \beta_{1k} + UWB * \beta_{2k} + IMU * \beta_{3k} + ANC * UWB * \beta_{3k} + ANC * IMU * \beta_{5k} + ANC^2 * \beta_{6k} + UWB^2 * \beta_{7k} + IMU^2 * \beta_{8k} + \varepsilon_{0k} \quad (20)$$

TABLE V. BOX-BENHNKEN DESIGN

System Configuration	EKF		UKF	
	MAPEX %	MAPEY %	MAPEX %	MAPEY %
No of Anchor	4,83448	4	4,85765	4,57386
UWB (Hz)	10	6,30748	10	5,14267
IMU (Hz)	100	99,9995	100	25
MAPE	8,50264	4,15705	8,08533	2,21299

EKF/UKF results in 5 UWB anchor are approximately the same in terms of the MAPE from BBD results which are given Table V. Considering 5 anchor configuration, the obtained results are shown in Fig. 4.

Shown in Fig. 5 and Fig. 6, REF is reference pattern LS is least squares, EKF is extended kalman filter and UKF is unscented kalman filter. actx and acty refer to the reference positions on the x and y axes, respectively.

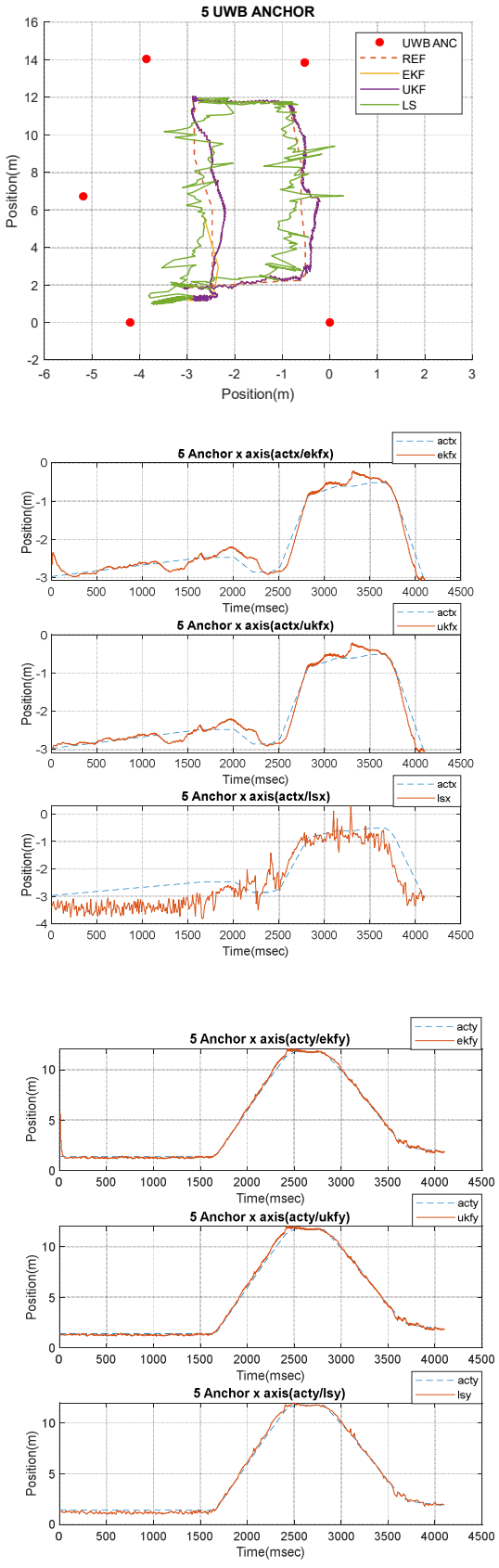

Fig. 6. Localization with 5 Anchors

In order to reduce error rates, EKF with six anchors is determined. EKF or UKF with a high-pass filter provides a significantly reduced error rate compared to positioning that is performed with UWB only. Considering the six anchor configuration, the obtained results are shown in Fig. 7.

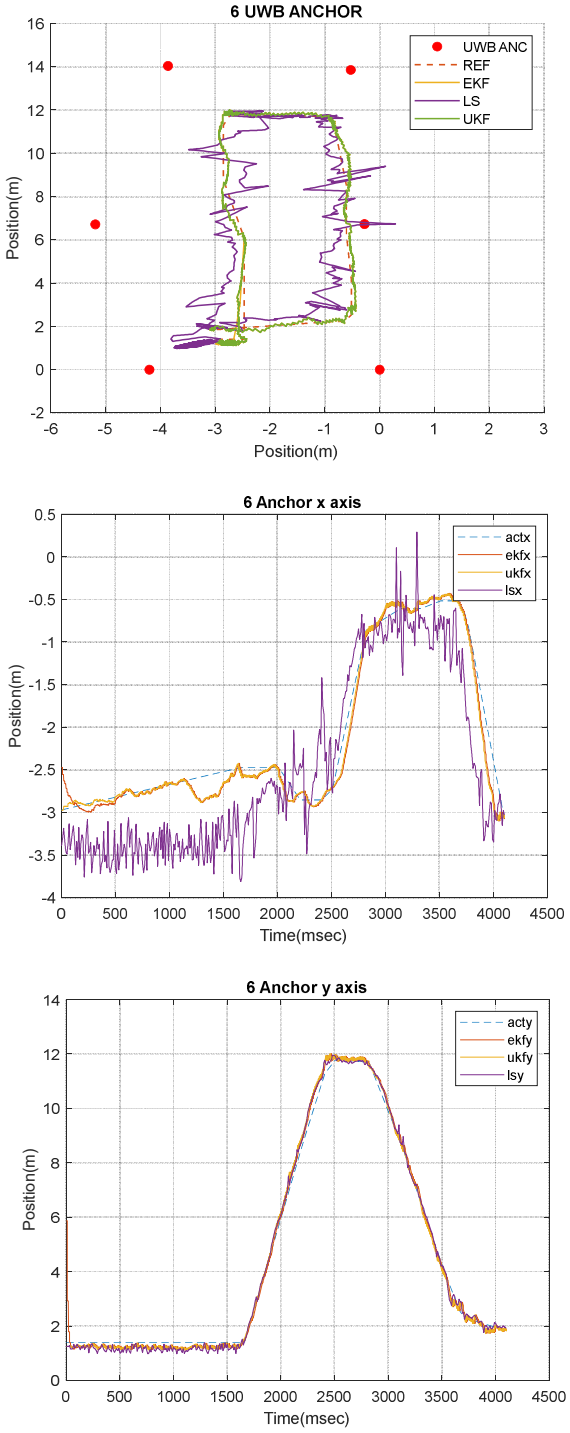

Fig. 7. Localization with 6 Anchors

V. Conclusion

This study analyses the application of Design of Experiments (DoE) and sensor fusion techniques for indoor navigation systems, specifically using UWB-IMU sensors along with estimation algorithms. When UWB is used for indoor navigation, some measurement mistakes occur due to environmental challenges like NLOS and multipath effects, leading to an increased error rate in position estimation. The application of sensor fusion is expected to mitigate these

errors. In contrast to existing literature, this study explores the impact of parameters such as IMU period, UWB usage, and the number of UWB anchors. Based on the experimental findings, optimal parameter configurations are determined, and linear regression analysis is performed to evaluate their effectiveness.

Distance measurements are performed based on TWR communication method between the UWB tag and anchor devices. These measurements are utilized for localization through the least squares method. Coordinate transformation is performed by using the ZYX Euler angle set for navigation frame movement of the data of the gyroscope and accelerometer that were derived from the IMU sensor. To improve the noisy data that comes from the IMU after the coordinate transformation, a high-pass filter is applied before feeding the data into EKF and UKF. In the application of EKF and UKF, the IMU data is used in predict equations, and UWB measurements are used in update equations. EKF and UKF is fed with the data that is derived from DoE under the NLOS environment. The estimated position and reference position data are shown in Table IV. MAPE results are compared.

The optimal parameter configuration value is calculated by using the BBD method. According to these results, system position tests are performed by using five UWB anchors, 100 Hz IMU period, and 10 Hz UWB period. According to the position tests, MAPEX value is found as %8,7658 in the EKF application and BBD and MAPEX was measured as %8,50264. The calculation that was made by BBD method is matched with the real test results. The MAPEX value is at acceptable levels for NLOS environment. However, to observe the impact of error rate on the anchor number, position tests are performed with six UWB anchors. It is observed that MAPEX value is decreased to %5 in the EKF application in position tests. These tests that were made with 6 UWB Anchor are repeated by using UWB sensors only. By using UWB, MAPEX value is measured as %31.2805 in the positioning performed by the least squares method. Thus, it is seen that sensor fusion algorithm improves (fixes) the error rate in position estimation under the NLOS environment.

In the next phase of this study, further experiments will be conducted to obtain UWB measurements under both line-of-sight (LOS) and non-line-of-sight (NLOS) environments. These additional experiments aim to achieve an optimal parameter configuration by increasing the number of system parameters.

REFERENCES

[1] L. Yao, Y. -W. A. Wu, L. Yao and Z. Z. Liao, "An integrated IMU and UWB sensor based indoor positioning system," 2017 International Conference on Indoor Positioning and Indoor Navigation (IPIN), Sapporo, Japan, 2017, pp. 1-8, doi: 10.1109/IPIN.2017.8115911.

[2] Y. Zhong, T. Liu, B. Li, L. Yang and L. Lou, "Integration of UWB and IMU for precise and continuous indoor positioning," 2018 Ubiquitous Positioning, Indoor Navigation and Location-Based Services (UPINLBS), Wuhan, China, 2018, pp. 1-5, doi: 10.1109/UPINLBS.2018.8559718.

[3] S. Jang, B. An, S. Yoon and K. Lim, "Research on the Indoor Environment Positioning Algorithm Using Sensor Fusion," 2023 International Conference on Electronics, Information, and Communication (ICEIC), Singapore, 2023, pp. 1-4, doi: 10.1109/ICEIC57457.2023.10049976.

[4] Z. Zuo, K. Li, P. Yang and S. Zheng, "Indoor UAV Integrated Navigation Technology Based on UWB and IMU," 2022 China Automation Congress (CAC), Xiamen, China, 2022, pp. 6594-6599, doi: 10.1109/CAC57257.2022.10055191.

[5] W. Guosheng, Q. Shuqi, L. Qiang, W. Heng, L. Huican, and L. Bing, "UWB and IMU System Fusion for Indoor Navigation," Chinese Control Conference (CCC), 2018 pp. 4946–4950. doi: 10.23919/ChiCC.2018.8483323.

[6] P. Dabove, V. Di Pietra, M. Piras, A. A. Jabbar and S. A. Kazim, "Indoor positioning using Ultra-wide band (UWB) technologies: Positioning accuracies and sensors' performances," 2018 IEEE/ION Position, Location and Navigation Symposium (PLANS), Monterey, CA, USA, 2018, pp. 175-184, doi: 10.1109/PLANS.2018.8373379.

[7] V. Krishnaveni B, S. Reddy K, R. Reddy P. "Indoor Tracking by Adding IMU and UWB using Unscented Kalman Filter", 2021, doi.org/10.21203/rs.3.rs-163258/v1

[8] H. Xing, Z. Chen, H. Yang, C. Wang, Z. Lin, and M. Guo, "Self-alignment MEMS IMU method based on the rotation modulation technique on a swing base," Sensors (Switzerland), vol. 18, 2018, doi: 10.3390/s18041178.

[9] J.Zhou, "Low-cost MEMS-INS/GPS Integration using Nonlinear Filtering Approaches," 2014,Available: https://www.researchgate.net/publication/241699864

[10] R. V. d. A. Lira and A. L. P. S. Campos, "Parameters optimization for rectangular and circular microstrip antennas using the Taguchi Method," 2017 SBMO/IEEE MTT-S International Microwave and Optoelectronics Conference (IMOC), Aguas de Lindoia, Brazil, 2017, pp. 1-5, doi: 10.1109/IMOC.2017.8121036.

[11] U. Demir and M. C. Aküner, "Using taguchi method in defining critical rotor pole data of LSPMSM considering the power factor and efficiency," Tehnicki Vjesnik, vol. 24, no. 2, pp. 347–353, Apr. 2017, doi: 10.17559/TV-20140714225453.

[12] U. Demir, "Improvement of the power to weight ratio for an induction traction motor using design of experiment on neural network," Electrical Engineering, vol. 103, no. 5, pp. 2267–2284, Oct. 2021, doi: 10.1007/s00202-020-01204-2.

[13] Kocabicak, Z. K. and Demir, U. "Design and optimization of an electromechanical actuator for the latch of a foldable vehicle seat" Materials Testing, vol. 62, no. 7, 2020, pp. 749-755. doi:10.3139/120.111539

[14] Demir, U. "IM to IPM design transformation using neural network and DoE approach considering the efficiency and range extension of an electric vehicle". Electr Eng 104, 1141–1152,2022. doi:10.1007/s00202-021-01378-3.